Chemical Science

ROYAL SOCIETY OF CHEMISTRY

EDGE ARTICLE

View Article Online
View Journal | View Issue

Cite this: *Chem. Sci.*, 2022, **13**, 11623

All publication charges for this article have been paid for by the Royal Society of Chemistry

Received 20th May 2022
Accepted 15th September 2022

DOI: 10.1039/d2sc02822k

rsc.li/chemical-science

Visible-light-induced indole synthesis *via* intramolecular C–N bond formation: desulfonylative C(sp^2)–H functionalization†

Quanzhe Li,[a] Xintao Gu,[a] Yin Wei*[a] and Min Shi *[ab]

Despite significant advances made on the synthesis of indole derivatives through photochemical strategies during the past several years, the requirement of equivalent amounts of oxidants, bases or other additional additives has limited their practical applications in the synthesis of natural products and pharmaceuticals as environment-friendly processes. Herein, we report LED visible-light-induced redox neutral desulfonylative C(sp^2)–H functionalization for the synthesis of *N*-substituted indoles with a broad scope through γ-fragmentation under mild conditions in the absence of any additional additive. The reaction mechanism paradigm has been investigated on the basis of deuterium labeling experiments, kinetic analysis, Hammett plotting analysis and DFT calculations.

Introduction

Indole motifs are privileged scaffolds found in many natural products[1] and biologically active compounds,[2] and therefore they have been a target of numerous methodology developments.[3] However, many of these developed methodologies are facing the lack of starting material availability and functional-group tolerance, resulting in restricted practicability or the requirement of high costs of starting materials. In general, starting from *ortho*-halogenated aniline derivatives, most of the synthetic methodologies had to use stoichiometric amounts of oxidants, bases or others as additional additives in the reaction under harsh reaction conditions, leading to the generation of undesired wastes[3b,g] (Scheme 1, Traditional Process). Furthermore, as for traditional intramolecular indole synthetic methodologies, although metal-catalyzed processes have been well developed,[3g,h,4] the use of prefunctionalized aniline derivatives is still required in most of the cyclization processes (Scheme 1, Traditional Process). Thus, the further development of new types of practical synthetic methods for the rapid construction of indole motifs is highly desired.[5]

Visible-light activated photoredox catalysis for the synthesis of indole derivatives has recently emerged as a novel reaction mode and an alternative to traditional processes for the synthesis of indole derivatives.[6] For example, Zheng's group[7] and Wu's group[8] delicately reported an intramolecular indole synthesis initiated by an efficient single electron oxidation of

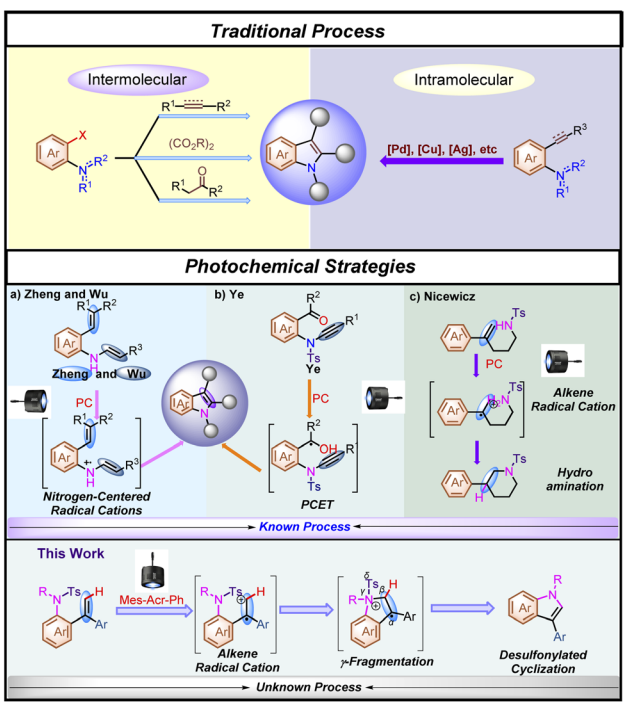

Scheme 1 Previous studies on the preparation of indole motifs and this work.

[a]*State Key Laboratory of Organometallic Chemistry, Center for Excellence in Molecular Synthesis, Shanghai Institute of Organic Chemistry, University of Chinese Academy of Science, Chinese Academy of Sciences, 345 Lingling Road, Shanghai 200032, China. E-mail: weiyin@sioc.ac.cn*

[b]*Key Laboratory for Advanced Materials and Institute of Fine Chemicals, School of Chemistry & Molecular Engineering, East China University of Science and Technology, 130 Meilong Road, Shanghai 200237, China. E-mail: mshi@mail.sioc.ac.cn*

† Electronic supplementary information (ESI) available. CCDC 2108706. For ESI and crystallographic data in CIF or other electronic format see https://doi.org/10.1039/d2sc02822k

the nitrogen atom using styryl aniline derivatives and *N*-aryl enamines, respectively under visible-light-irradiation (Scheme 1a, Photochemical Strategy). In addition, sulfonamides, as robust protecting groups, are easy to purify and are very stable under various reaction conditions.[9] Recently, desulfonylation of tosyl amides through catalytic photoredox cleavage processes has attracted much attention from organic chemists.[10] In 2020, Ye and co-workers[11] reported an outstanding study of ynamide Smiles rearrangement triggered by visible-light-mediated regioselective ketyl–ynamide coupling, which enables facile access to a variety of valuable 2-benzhydrylindoles or isoquinolines with a broad substrate scope in generally good yields under mild reaction conditions (Scheme 1b, Photochemical Strategy). On the other hand, Fukuzumi acridinium salts ($*E_{1/2red} > +1.60$ V *vs.* SCE),[12] as excellent photo-oxidation catalysts in the excited state, have been extensively reported to oxidize alkenes through single-electron oxidation. In this respect, Nicewicz,[13] Glorius[14] and others[15] have demonstrated that alkene radical cations are susceptible to highly regioselective nucleophilic attack, and because this step does not involve a discrete nucleophile–catalyst interaction, they are relatively agnostic toward the identity of the nucleophilic reaction partner (Scheme 1c, Photochemical Strategy). On the basis of these research backgrounds, we envisaged that if an appropriate organic radical intermediate and desulfonylated elimination could be merged together, a redox neutral process might be able to be established as a brand-new alternative photochemical platform for indole synthesis through γ-fragmentation. Herein, we wish to disclose how this hypothesis was translated into experimental reality, enabling a desulfonylated process as an additional additive-free and step-economic strategy for the synthesis of indole (Scheme 1, this work).

To verify our working hypothesis, we initiated our study by using tosylated biphenylalkene derivative **1a** (0.1 mmol, 1.0 equiv.) as a substrate, xanthone (5.0 mol%) as a photosensitizer and CH_3CN as the solvent under an argon atmosphere upon 12 W 365 nm LED light irradiation for 12 hours. To our delight, the desired indole product **2a** was produced in 15% yield (Table 1, entry 1). Using thioxanthone and *fac*-Ir(ppy)$_3$ as photocatalysts did not afford **2a** at all (Table 1, entries 2 & 3). Since the acridinium derivative had a strong absorption band in the visible region (λ = 430 nm) along with the high oxidation

Table 1 Optimization of reaction conditions[ab]

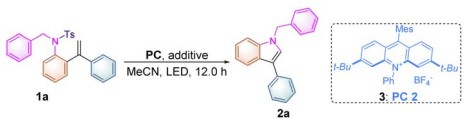

Entry[a]	PC	PC (mol%)	Additive	Solvent	LED	Yield[b] (%)
1	Xanthone	5.0	—	MeCN	365 nm	15
2	Thioxanthone	5.0	—	MeCN	365 nm	—
3	*fac*-Ir(ppy)$_3$	5.0	—	MeCN	365 nm	—
4	**PC 1**	5.0	—	MeCN	365 nm	79
5	**PC 2**	5.0	—	MeCN	365 nm	88
6	**PC 3**	5.0	—	MeCN	365 nm	—
7	**PC 4**	5.0	—	MeCN	365 nm	—
8	**PC 2**	5.0	—	MeCN	385 nm	90
9	**PC 2**	5.0	—	MeCN	Blue LED (100 W)	88
10	**PC 2**	1.0	—	MeCN	385 nm	83
11	**PC 2**	**2.0**	—	**MeCN**	**385 nm**	**91 (90)**[c]
12	**PC 2**	3.0	—	MeCN	385 nm	81
13	**PC 2**	4.0	—	MeCN	385 nm	83
14	**PC 2**	2.0	—	THF	385 nm	<5
15	**PC 2**	2.0	—	DMF	385 nm	—
16	**PC 2**	2.0	—	DCM	385 nm	51
17[d]	**PC 2**	5.0	DIPEA	MeCN	385 nm	29
18[d]	**PC 2**	5.0	Hantzsch ester	MeCN	385 nm	—
19	—	—	—	MeCN	385 nm	—
20[e]	**PC 2**	2.0	—	MeCN	385 nm	—
21[f]	**PC 2**	2.0	—	MeCN	385 nm	82[c]

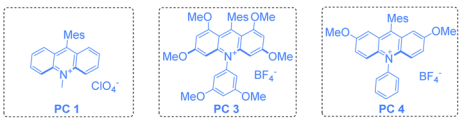

[a] Reaction conditions: **1a** (0.1 mmol) and **PC** (*x* mol%) were added to degassed MeCN (2.0 mL) under an Ar atmosphere for 12.0 h, in a sealed tube using LED light irradiation. [b] NMR yield using 1,3,5-trimethoxybenzene as an internal standard. [c] Yield of the isolated products. [d] Additive (0.2 mmol) was used. [e] Under dark conditions. [f] A scale-up reaction with 1.0 mmol of **1a**.

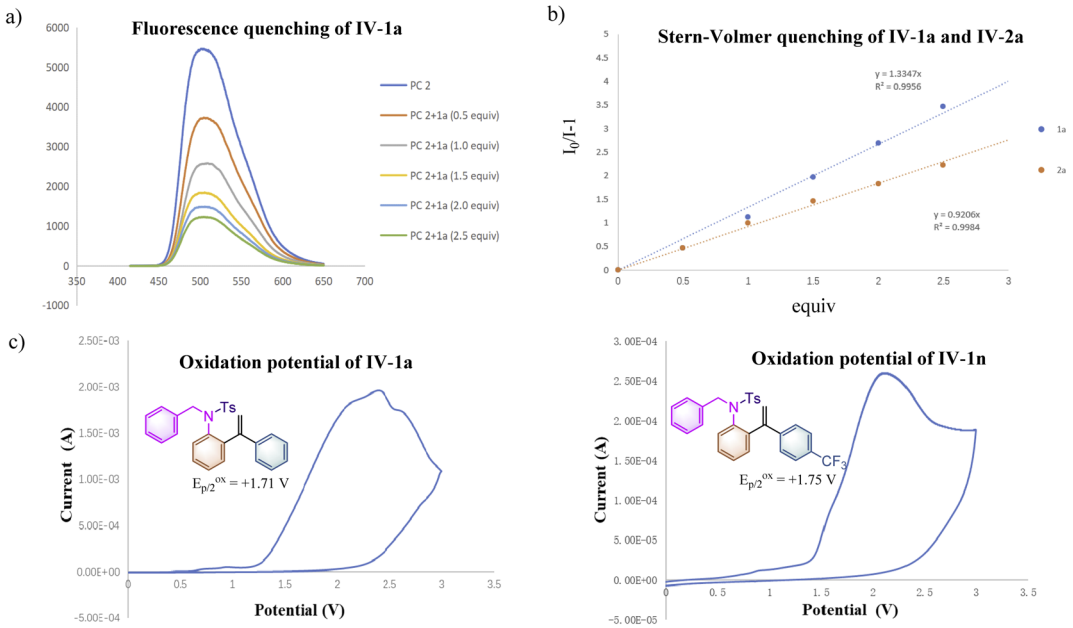

Scheme 2 Mechanistic studies. (a) Solution of **PC 2** (5.0×10^{-3} M) was added to **1a** (1.0 M, 0.5 equiv. as gradient) in dry MeCN upon excitation at 415 nm. (b) Solution of **PC 2** (5.0×10^{-3} M) was added to **1a** and **2a** (1.0 M, 0.5 equiv. as gradient), respectively in dry MeCN upon excitation at 415 nm. (c) A solution of the substrate **1** in MeCN (0.2 M) was tested with 0.2 M Bu_4NPF_6 as the supporting electrolyte, using glassy carbon as the working electrode, Pt as the counter electrode, and a saturated calomel electrode reference electrode. Scan rate = 0.1 V s^{-1}, 2 sweep segments, a sample interval of 0.001 V.

potential in the excited state, acridinium **PC 1** ($E_{1/2red}^* = +2.06$ V *vs.* SCE)[12] was used as the photocatalyst in this reaction, giving **2a** in 79% yield (Table 1, entry 4). This uplifting result demonstrated that it was feasible to initiate the reaction through oxidation of the alkene moiety in **1a** ($E_{1/2}^{ox} = +1.71$ V *vs.* SCE) (for details see Scheme 2c or ESI, at page S43†) upon SET with the excited state of $MesAcr^+$*, resulting in the formation of the alkene radical cation to trigger the intramolecular nucleophilic attack of the tosylated amino moiety, giving the desired indole product **2a**. Furthermore, using **PC 2** ($E_{1/2red}^* = +2.08$ V *vs.* SCE)[12] as a photocatalyst provided **2a** in 88% (Table 1, entry 5). However, **PC 3** ($E_{1/2red}^* = +1.65$ V *vs.* SCE)[12] and **PC 4** ($E_{1/2red}^* = +1.90$ V *vs.* SCE),[12] which had lower redox potentials, were not suited to this transformation of **1a** (Table 1, entries 6 & 7). Screening of LED light sources revealed that 385 nm LED light was the best one for the production of **2a** (Table 1, entries 8 & 9). Subsequently, the examination of photocatalyst loading indicated that the use of 2.0 mol% **PC 2** is the most suitable condition, delivering **2a** in the highest yield of 91% along with 90% yield of the isolated products (Table 1, entries 10–13). As for solvent effect studies, it was found that THF and DMF were not productive in this transformation (Table 1, entries 14 & 15) and using DCM as the solvent gave **2a** in 51% yield (Table 1, entry 16). Moreover, we also found that the yield of **2a** significantly decreased in the presence of sacrificial reducing agents such as Hantzsch ester and DIPEA (Table 1, entries 17 & 18). The control experiments illustrated that both the photocatalyst and light irradiation were requisite for the generation of indole product **2a** (Table 1, entries 19 & 20) (for more information, see Tables S1–S3 in the ESI†). A scale-up reaction could be performed with 1.0 mmol of **1a**, affording **2a** in 82% yield, *i.e.*, 232 mg (Table 1, entry 21) (see ESI at page S30†).

With the optimized conditions identified, the substrate scope of this reaction has been examined with a wide range of substrates **1** and it was found that most of them underwent this transformation successfully, providing the desired products in good yields (Table 2). As for introducing substituents onto the benzene ring connected both to the alkene and sulfonated moieties, we found that substrates **1c–g** bearing electron-withdrawing or -donating substituents, such as halogen atoms, fluorine or methyl or *tert*-butyl groups, turned out to be applicable under the optimal reaction conditions, affording the desired products **2c–g** in good to excellent yields ranging from 75% to 88%. Surprisingly, in the case of substrate **1b** having a strongly electron-donating methoxyl group in the benzene ring, no reaction occurred, which is quite different from the Stephenson's observation,[16] in which the electron-rich phenyl ring, with decreasing oxidation potential of styrene, would promote the reaction. For substrate **1b**, the BET (back electron transfer) process[17] may easily occur because of the lower barrier of the SET process in the initial state in this reaction, indicating that no reaction could take place along with complete recovery of the starting materials. Replacing the benzene ring by a naphthalene unit gave the corresponding product **2h** in 79% yield. Subsequently, we expanded the substrate scope of the substituted benzene ring connected only to the alkene moiety and found that introducing substituents such as methyl or ethyl groups, halogen atoms, fluorine groups or trifluoromethyl groups at 2′-, 3′-, and 4′-positions of the benzene ring turned out to be compatible, furnishing the desired products **2i–p** in 76–

Table 2 Substrate scope of **1**[ab]

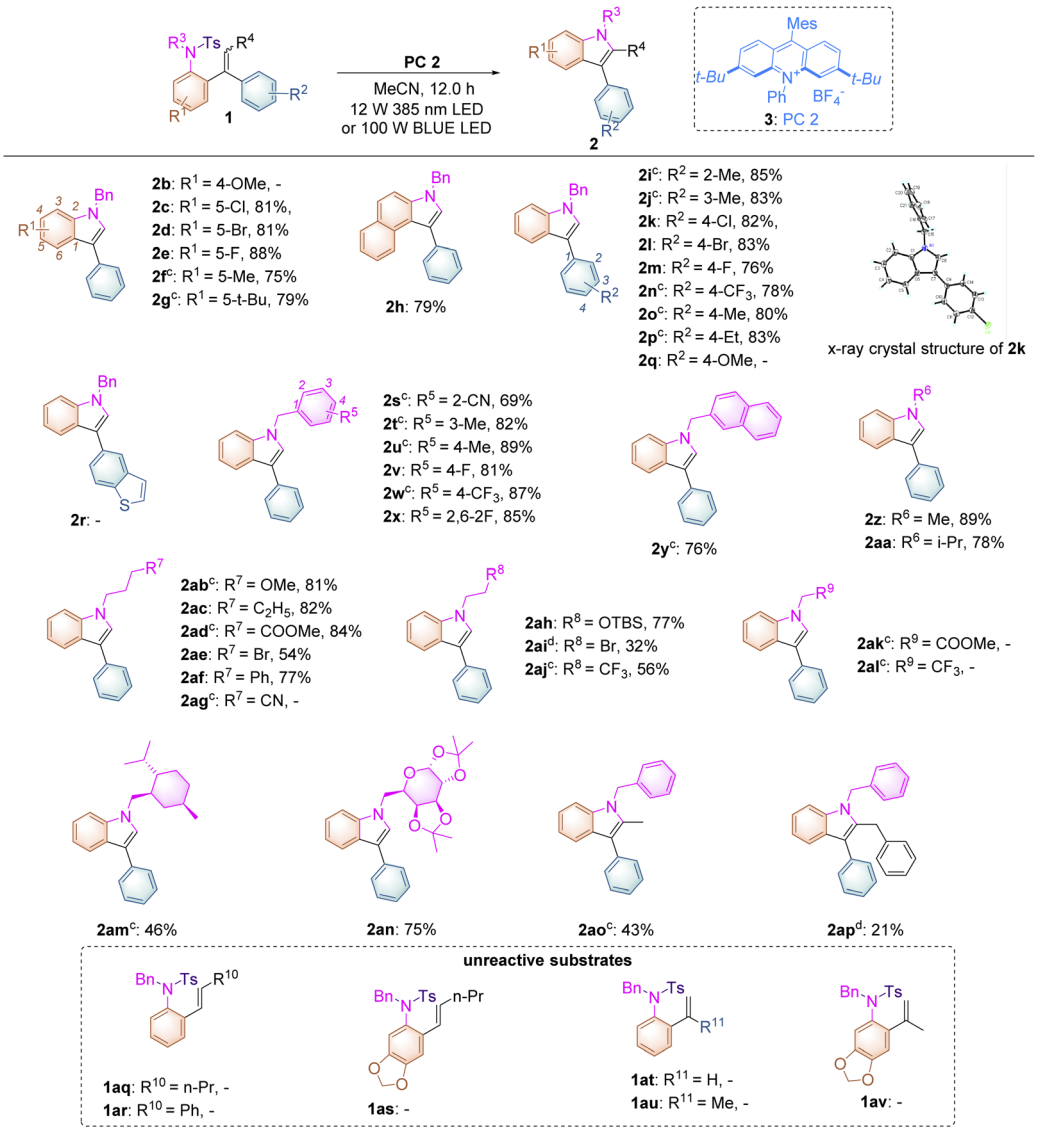

[a] Reaction conditions: **1** (0.1 mmol) and **PC 2** (2.0 mol%) were added to degassed MeCN (2.0 mL) under an Ar atmosphere for 12.0 h, in a sealed tube using 385 nm LED light irradiation. [b] Yield of the isolated products. [c] Reaction conditions: **1a** (0.1 mmol) and **PC 2** (2.0 mol%) were added to degassed MeCN (2.0 mL) under an Ar atmosphere for 24.0 h, in a sealed tube using 100 W blue light irradiation. [d] Reaction conditions: **1** (0.1 mmol) and **PC 2** (2.0 mol%) were added to degassed DCM (2.0 mL) under an Ar atmosphere for 24.0 h, in a sealed tube using 100 W blue light irradiation.

85% yields. The structure of **2k** had been unambiguously determined by X-ray diffraction as shown in Table 2 and the corresponding CIF data are presented in the ESI.† As for substrate **1q** having an electron-rich aromatic ring and substrate **1r** bearing a heteroaromatic ring, no reactions occurred as well similar to that of **1b** along with complete recovery of the starting materials. The tethered benzyl group in substrates **1s–x** has also been examined and we found that when introducing cyano, methyl or trifluoromethyl groups as well as fluorine atoms onto its benzene ring, the reactions proceeded smoothly, delivering the desired products **2s–x** in 69–89% yields. The benzene ring could be replaced by a naphthyl group, giving **2y** in 76% yield. Besides the benzyl group, R^6 could be a methyl group (substrate **1z**, R^6 = Me) or an isopropyl group (substrate **1aa**, R^6 = *i*-Pr), affording the desired products **2z** and **2aa** in 89% and 78% yields, respectively. As the nucleophilicity of the tosylated nitrogen atom is also an essential factor for this photo-induced cyclization, the tethered alkyl effect based on the length of the carbon chain along with its electronic effect has also been investigated. Substrates **1ab–af**, in which R^7 = OMe, C_2H_5, CO_2Me, Br, or Ph bearing three $-CH_2-$moieties, were tolerated under the optimal reaction conditions, affording the desired products **2ab–af** in moderate to good yields ranging from 54% to 84%. However, in the case of substrate **1ag** (R^7 =

CN), we failed to get the desired product **2ag** after several attempts under different reaction conditions, presumably due to that the aliphatic cyano group may interact with the excited photocatalyst to impair the reaction proceeding or the electronic nature of the aliphatic cyano group may enhance its oxidation potential, disturbing the SET process between the excited photocatalyst and **1ag**. Furthermore, for substrates **1ah–aj**, in which R^8 = OTBS, Br, or CF_3 bearing two $-CH_2-$ moieties, the reactions became less facile under the standard conditions, affording the corresponding products **2ah–aj** in 32–77% yields. It should be noted that substrates **1ak** (R^9 = COOMe) and **1al** (R^9 = CF_3) bearing one $-CH_2-$ moiety did not undergo the desired process to give the indole product, indicating that the inductive effect plays a role in the nucleophilicity of the tosylated nitrogen atom and the electron-withdrawing CO_2Me or CF_3 at the β position of the nitrogen atom can decrease its nucleophilicity. In the meantime, for substrate **1am** having a menthol skeleton and substrate **1an** bearing a modified sugar group, the reactions were also tolerated, delivering the corresponding products **2am** and **2an** in 46% and 75% yields, respectively. Furthermore, using substrates **1ao** (*Z*/*E* = 1/0.9) and **1ap** (*Z*/*E* = 1/0.4) in the reaction showed that only the *E* configuration was reactive along with full recovery of unreactive substrates with the *Z*-configuration because after the reaction completion, the remaining substrates **1ao** and **1ap** were determined to have the *Z*-configuration upon NOE spectroscopic analysis (see ESI at page S58†). The *Z–E* isomerization of anethole reported in Stephenson's work,[16] in which the initial rate of (*Z*)-anethole isomerization was much faster than that of (*E*)-anethole isomerization at the photostationary state, could not be identified in this reaction process. Unfortunately, styrene-type substrates **1aq–av** were incompatible in this transformation.

To further broaden the substrate scope on this newly developed visible-light-induced photochemical synthetic methodology and to carry out mechanistic investigations, substrates **1aw–aak**, having different *N*-protecting R groups, were studied in this transformation (Table 3). When substrate **1aw** (R^1 = H) was employed, the desired product **2a** was obtained in 82% yield. Substrates **1ax–az**, in which the fluorine atom was introduced at the 2-, 3-, and 4-positions of the benzene ring, afforded **2a** in increased yields of 37%, 64% and 98% respectively perhaps due to the steric and electronic effects under the standard conditions. For substrates **1aaa–aaw**, in which R^1 = 4-Cl, 4-OMe, 4-CF_3, 4-NO_2, 4-CN, the desired product **2a** could also be obtained in 35–95% yields. Replacing the benzene ring by a naphthalene moiety or a thiophene moiety provided **2a** in 85% and 71% yields, respectively. Moreover, substrates **1aah** (R = Ms) and **1aai** (R = Tf) were also compatible in this methodology, affording **2a** in 85% and 60% yields. However, substrates **1aaj** (R = Ac), **1aak** (R = $CF_3C(O)$), **1aal** (R = Boc) and **1aam** (R = H) were not applicable in this process, indicating that the use of a sulfonyl group as a *N*-protecting group is essential in this photochemical transformation.

To further clarify the interaction details between the photocatalyst and substrate **1a**, the fluorescence quenching experiment of **PC 2** (5.0×10^{-3} M) with **1a** (1.0 M, 0.5 equiv. as a gradient) was performed and the emission of **PC 2** was effectively quenched by **1a** as shown in Scheme 2a. The Stern–Volmer analytical results of **PC 2** with substrate **1a** and product **2a** are depicted in Scheme 2b, suggesting that **1a** can more efficiently quench the emission of **PC 2** than that of **2a**. To get more accurate results, Stern–Volmer experiments of compounds **1a** and **2a** were repeated at a lower concentration using **PC 2** (5.0×10^{-5} M) and similar results were obtained (for more details, see ESI at pages S38–S42†). The oxidation potentials of **1a** and **1n** were measured as $E^{ox}_{p/2}$ = +1.71 V *vs.* SCE and $E^{ox}_{p/2}$ = +1.75 V *vs.* SCE as shown in Scheme 2c, suggesting that the inductive effect on the benzene ring could slightly increase the oxidation potential of substrate **1** (for more details, see ESI, at page S43†). It is noteworthy that the reaction rate of **1n** having a CF_3 group at the *para*-position of the benzene ring was similar to that of **1o** having a Me group, while both of them are much slower than that of substrate **1a** (see ESI at page S52 and S55† for more details). As measured above, the reaction rate of **1n** is more sluggish than that of **1a** under identical conditions probably owing to its higher oxidation potential. As for substrate **1o**, electronic distribution on the styrene moiety in the transition state may be the key point resulting in the deceleration of the reaction rate of **1o**. The relatively high reaction rate of substrate **1a** may imply the presence of a significant chain process. To further verify our hypothesis, the quantum yields of the reactions of **1a**, **1n** and **1o** under the standard conditions were measured as 1.77, 0.18 and 0.17, respectively (see ESI, at page S35† for more details). The results indicate that the photochemical chain process indeed exists in the reaction of **1a**; a possible radical chain process cannot be excluded in the reactions of **1n** and **1o**, since it can be a consequence of a highly inefficient initiation process or a short-lived chain propagation process due to the substituent effect.[18] Overall, this reaction may involve an inefficient radical chain process.

As shown in Scheme 3, the deuterium labeled kinetic experiment was conducted to gain information on the rate-

Table 3 The study of the leaving sulfonyl group and the other *N*-protecting groups in **1aw–aak**[ab]

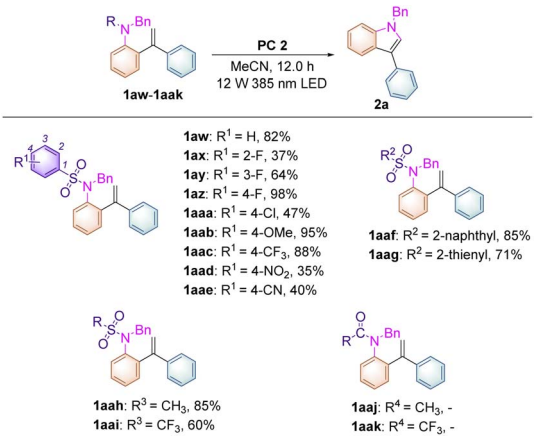

[a] Reaction conditions: **1aw–aak** (0.1 mmol) and **PC 2** (2.0 mol%) were added to degassed MeCN (2.0 mL) under an Ar atmosphere for 12.0 h, in a sealed tube using 385 nm LED light irradiation. [b] NMR yield using 1,3,5-trimethoxybenzene as an internal standard.

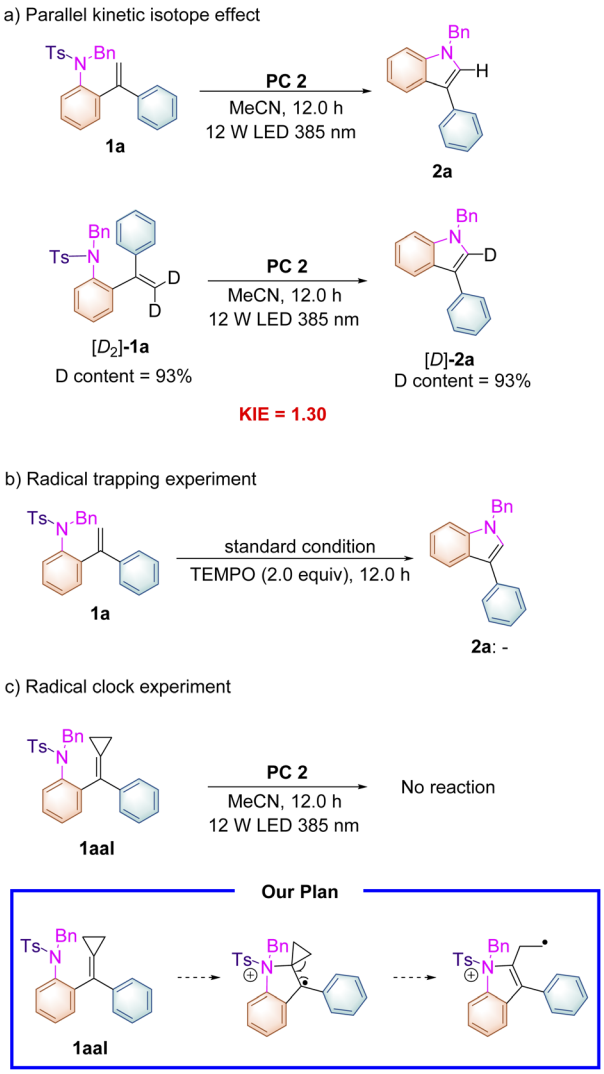

Scheme 3 (a) Parallel kinetic isotope effects, (b) radical trapping experiments, and (c) radical clock experiments.

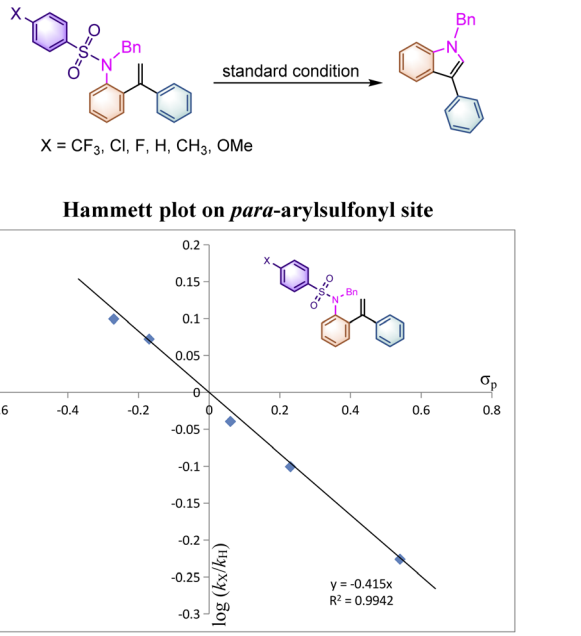

Scheme 4 Parallel substituent effect on the *para*-arylsulfonyl site.

determining step. The kinetic isotope effect of this reaction was measured on the basis of parallel experiments, and a k_H/k_D value of 1.30 was obtained (Scheme 3a), which suggested that the C–H cleavage might not be involved in the turnover-limiting process. Adding radical scavenger 2,2,6,6-tetramethyl-1-piperidinyloxy (TEMPO) (2.0 equiv.) into the reaction system completely suppressed the reaction proceeding and none of the cyclized products was detected under the standard conditions (Scheme 3b). Subsequently, a radical clock experiment with a cyclopropane-modified alkene **1aal** as a substrate was carried out under the standard conditions. Unfortunately, we found that no reaction occurred presumably due to the steric effect (Scheme 3c). This substrate was designed on the basis of our proposed reaction mechanism shown in Scheme 5, in which a radical intermediate **5a** was involved as a key radical species.

To better indicate the influence of the electronic characteristics of the arylsulfonyl moiety on this reaction, the Hammett effect was examined in this system. A set of parallel reactions of **1aab**, **1a**, **1aw**, **1az**, **1aaa** and **1aac** bearing various substituents on the benzene ring were carried out under identical conditions. As listed in Table 4, the reaction rates of substrates **1aab** and **1a** with electron-donating substituents on the *para*-phenylsulfonyl site are found to be faster than those of **1az**, **1aaa** and **1aac**, where the electron-withdrawing substituents decelerated the reaction rate. Plotting $\log(k_X/k_H)$ *versus* σ_p gave an excellent linear plot with ρ_p being −0.415, indicating that a positively charged intermediate should be generated during the reaction process (Scheme 4). This result suggested that the reaction initiates from the nucleophilic attack of the nitrogen atom to the alkene moiety to generate a cationic species. As for the rate constants of 4′-substituted substrates **1a**, **1l**, **1n** and **1o** measured (see ESI at page S50† for more details), even if the spin-delocalization effect of the substituents was taken into account using the dual parameter equation $\log(k_X/k_H) = \rho^X\sigma^X + \rho^{\bullet}\sigma^{\bullet}$, neither Jiang's[19] σ_{mb} and $\sigma_{JJ}^{\bullet}$ scales nor Creary's[20] radical scale $\sigma_c^{\bullet}$ gave a linear correlation presumably due to the discrepancy of electronic distribution on the alkene moiety in the transition state, implying that the radical cationic intermediate may be involved in this transformation rather than a simple radical process.

The DFT calculations were conducted to further clarify the plausible reaction pathways. All calculations have been performed at the SMD/B3LYP/6-311+G(d,p)//B3LYP/6-31G(d) level with the Gaussian 16 program.[21] The solvation Gibbs free energy profile in acetonitrile for the suggested reaction pathway is shown in Scheme 5a (see ESI at page S268† for the details). The excited state of **PC 2** ($E_{p/2}^{red} = +2.08$ V *vs.* SCE) can facilitate the conversion of **1a** ($E_{p/2}^{ox} = +1.71$ V *vs.* SCE) to generate **1a**$^{\bullet+}$ *via* SET. The analysis of spin density shows that some amounts of spin densities are delocalized across nitrogen and carbon centers (0.358 and 0.228)[22] and the rest of the spin densities are delocalized on aryl groups. Subsequently, **1a**$^{\bullet+}$ undergoes cyclization

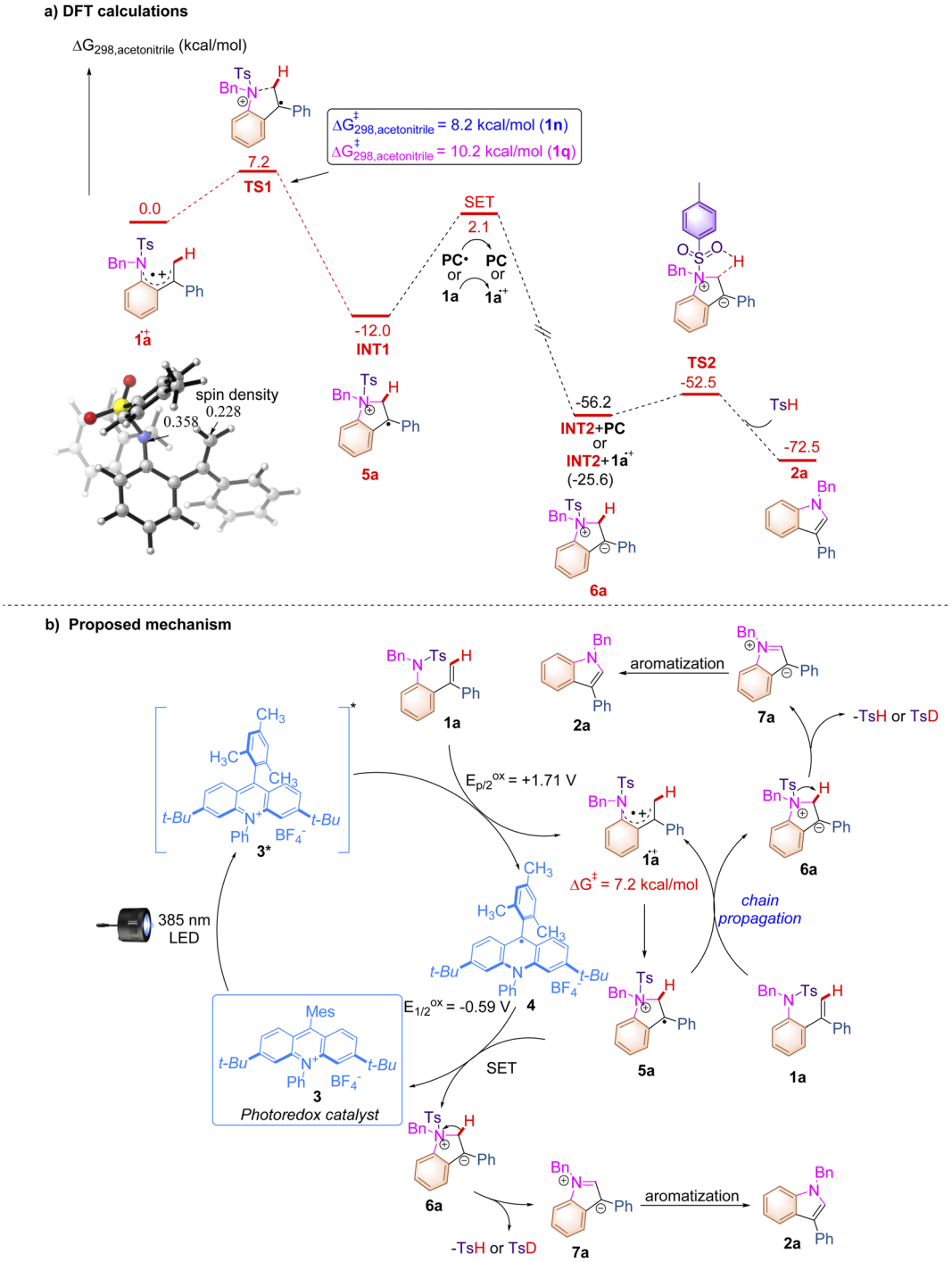

Scheme 5 (a) DFT calculations and (b) proposed reaction mechanism.

via **TS1** with an energy barrier of 7.2 kcal mol^{-1} to form a radical cation intermediate **INT1**, which is an exothermic process (ΔG = −12.0 kcal mol^{-1}). The energy barriers for cyclization with respect to substrates **1n** and **1q** are 8.2 kcal mol^{-1} and 10.2 kcal mol^{-1} (for details, see ESI at page S277†), which are in line with the experimental results that show that the reaction rate of **1n** is slower than that of **1a** and **1q** cannot undergo this reaction. The intermediate **INT2** is generated through a SET process with an energy barrier of 14.1 kcal mol^{-1} between **INT1** and **PC**$^{\cdot+}$ or between **INT1** and **1a**, which is a highly exothermic process and indicates that the radical chain process shown in Scheme 5b is thermodynamically favorable and has a possibility to take place. The intermediate **INT2** exists as a close ion pair. The **Ts**$^{-}$ anion moiety in **INT2** promotes deprotonation to give product **2a** and release TsH through a low activation barrier of 3.7 kcal mol^{-1}, which agrees with the result of the KIE

Table 4 Rate constant K_X, relative rates $\log(k_X/k_H)$ with the σ_p scale on the *para*-arylsulfonyl site

Subtituent	k_X	k_X/k_H	$\mathrm{Log}(k_X/k_H)$	σ_p
OMe	1.388	1.2572	0.0994	−0.27
CH_3	1.304	1.1812	0.0723	−0.17
H	1.104	—	—	—
F	1.008	0.9130	−0.0395	0.06
Cl	0.876	0.7935	−0.1005	0.23
CF_3	0.656	0.5942	−0.2261	0.54

experiment, indicating that the C–H cleavage is not involved in the turnover-limiting process. The experimentally observed KIE (1.3) suggested the potential normal secondary KIE effect, which usually implies a reaction from the sp^3–sp^2 ground-state to a transition-state in the rate-determining step. However, this photochemical reaction may not follow the normal rule since it involves the photoexcitation and SET processes which require higher energies than other steps. Based on the aforementioned experimental results and the detailed mechanistic investigations, we proposed a plausible reaction mechanism paradigm for this photochemical transformation (Scheme 5b). First, photoexcitation of acridinium salt **3** affords a highly oxidizing excited state $MesAcrPh^{+}$* ($^*E_{1/2red} = +2.06$ V *vs.* SCE), which is reductively quenched by substrate **1a**, furnishing radical cationic species **1a**$^{\cdot+}$ and acridine radical **4**. The intramolecular nucleophilic attack of the nitrogen atom to the alkene moiety in **1a**$^{\cdot+}$ affords cyclized radical cationic intermediate **5a** with an energy barrier of 7.2 kcal mol^{-1}, which undergoes a SET process with acridine radical **4** to deliver a zwitterionic intermediate **6a** along with the regeneration of acridinium salt **3** in the closed catalytic loop. The elimination of TsH (or TsD) from **6a** provides another zwitterionic intermediate **7a**, which undergoes a subsequent aromatization to furnish the desired indole product **2a**. Given the fact that the quantum yield of this reaction has been detected as 1.77, a chain process, in which **5a**$^{\cdot+}$ acts as an oxidant for another molecule of **1a** to produce **6a** and **1a**$^{\cdot+}$, takes place to afford **2a** as well through the same intermediate **7a**. The formation of TsH (or TsD) has been confirmed by Mass spectroscopy (see ESI at page S57†). As for the multistep process, it should be emphasized here that the kinetics of this reaction is probably related to both cyclization (**1a**$^{\cdot+}$ to **5a**) and SET (**5a** to **6a**) processes which are defined as rate determining steps.[23]

The *N*-benzyl substituted indole product **2a** can be easily transformed to the corresponding unsubstituted indole upon treatment with *t*-BuOK/DMSO and molecular oxygen at room temperature according to the previous literature (Scheme 6).[24] The compound **8a** itself (3-phenylindole) is a biologically active substance, which can be used as an antimicrobial active compound toward many fungi and Gram-positive bacteria. For instance, it inhibits the growth of *Aspergillus niger* at the 5 pg mL^{-1} level and can also suppress spore germination at 50 μg mL^{-1}.[25] Moreover, **8a** can be transformed to **9a** upon treatment with 2-chloroethylamine hydrochloride under basic conditions, which can be further converted into indole-fused CF_3-piperazine derivative **10a** through a Pictet–Spengler reaction

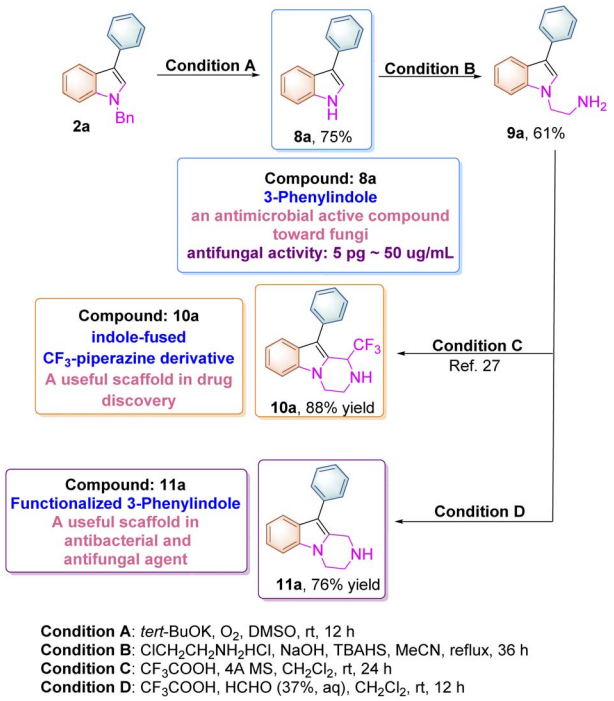

Scheme 6 Synthetic routes to bioactive indole compounds.

according to the previous literature.[26,27] In addition, a new pyrazino-indole derivative **11a** was also synthesized in 76% yield in this paper as shown in Scheme 6. These pyrazino-indole derivatives have been recognized as antibacterial and antifungal agents in drug discovery.[28]

Conclusions

In conclusion, we have explored a novel visible-light-induced photocatalytic synthetic methodology for the production of *N*-substituted indole products **2** through γ-fragmentation using acridinium salt **PC 2** as the photocatalyst and *N*-sulfonated arylalkene derivatives **1** as substrates under mild conditions without any additional additive. The investigation on the substituent effects with regard to the sulfonyl leaving groups disclosed that the desulfonylative reaction initiates from the intramolecular nucleophilic attack of the nitrogen atom to the alkene moiety of the radical cationic species of **1**. DFT calculations and kinetic experiments revealed that both cyclization (**1a**$^{\cdot+}$ to **5a**) and SET (**5a** to **6a**) processes are rate determining steps. A radical chain process was also involved in this reaction considering that the quantum yield is 1.77 and a light source is necessary. All of these results represent a robust and potentially useful strategy for the synthesis of indoles and will inspire further development in the synthesis of nitrogen atom-containing heterocycles under redox neutral conditions along with exploitation of the versatility of photoredox catalytic processes. The exploration of this photoinduced synthetic strategy in the synthesis of natural products or crucial pharmaceutical molecules and other complicated systems is currently under investigation.

Conflicts of interest

There are no conflicts to declare.

Data availability

Experimental and DFT computational data are available free of charge in ESI† section of this article.

Author contributions

Shi, M. directed the project and revised the manuscript. Li, Q. Z. and Gu, X. T. wrote the manuscript and carried out the reactions. Wei, Y. checked the spectroscopic data and carried out the DFT calculations.

Acknowledgements

We are grateful for the financial support from the National Natural Science Foundation of China (21372250, 21121062, 21302203, 20732008, 21772037, 21772226, 21861132014, 91956115 and 22171078), the project supported by the Shanghai Municipal Science and Technology Major Project (Grant No. 2018SHZDZX03) and the Fundamental Research Funds for the Central Universities 222201717003.

References

1 (*a*) L. Li, Z. Chen, X. Zhang and Y. Jia, *Chem. Rev.*, 2018, **118**, 3752–3832; (*b*) I. S. Marcos, R. F. Moro, I. Costales, P. Basabe and D. Díeza, Sesquiterpenyl indoles, *Nat. Prod. Rep.*, 2013, **30**, 1509–1526; (*c*) A. J. Kochanowska-Karamyan and M. T. Hamann, *Chem. Rev.*, 2010, **110**, 4489–4497; (*d*) M. Ishikura and K. Yamada, *Nat. Prod. Rep.*, 2009, **26**, 803–852; (*e*) S. E. O'Connor and J. J. Maresh, *Nat. Prod. Rep.*, 2006, **23**, 532–547; (*f*) M. Somei and F. Yamada, *Nat. Prod. Rep.*, 2005, **22**, 73–103; (*g*) M. Somei and F. Yamada, *Nat. Prod. Rep.*, 2004, **21**, 278–311; (*h*) D. L. Boger, C. W. Boyce, R. M. Garbaccio and J. A. Goldberg, *Chem. Rev.*, 1997, **97**, 787–828.

2 (*a*) T. P. Pathak, K. M. Gligorich, B. E. Welm and M. S. Sigman, *J. Am. Chem. Soc.*, 2010, **132**, 7870–7871; (*b*) S.-M. Li, *Nat. Prod. Rep.*, 2010, **27**, 57–78; (*c*) R. Ragno, A. Coluccia, G. L. Regina, G. D. Martino, F. Piscitelli, A. Lavecchia, E. Novellino, A. Bergamini, C. Ciaprini, A. Sinistro, G. Maga, E. Crespan, M. Artico and R. Silvestri, *J. Med. Chem.*, 2006, **49**, 3172–3184; (*d*) A. D. Napper, J. Hixon, T. McDonagh, K. Keavey, J.-F. Pons, J. Barker, W. T. Yau, P. Amouzegh, A. Flegg, E. Hamelin, R. J. Thomas, M. Kates, S. Jones, M. A. Navia, J. O. Saunders, P. S. DiStefano and R. Curtis, *J. Med. Chem.*, 2005, **48**, 8045–8054; (*e*) G. C. G. Pais, X. Zhang, C. Marchand, N. Neamati, K. Cowansage, E. S. Svarovskaia, V. K. Pathak, Y. Tang, M. Nicklaus, Y. Pommier and T. R. J. Burke, *J. Med. Chem.*, 2002, **45**, 3184–3194.

3 (*a*) L. Ackermann, *Acc. Chem. Res.*, 2014, **47**, 281–295; (*b*) M. Inman and C. J. Moody, *Chem. Sci.*, 2013, **4**, 29–41; (*c*) S. Cacchi and G. Fabrizi, *Chem. Rev.*, 2011, **111**, PR215–PR283; (*d*) B. Ganem, *Acc. Chem. Res.*, 2009, **42**, 463–472; (*e*) D. Ma and Q. Cai, *Acc. Chem. Res.*, 2008, **41**, 1450–1460; (*f*) J. M. Richter, Y. Ishihara, T. Masuda, B. W. Whitefield, T. Llamas, A. Pohjakallio and B. S. Baran, *J. Am. Chem. Soc.*, 2008, **130**, 17938–17954; (*g*) G. R. Humphrey and J. T. Kuethe, *Chem. Rev.*, 2006, **106**, 2875–2911; (*h*) S. Cacchi and G. Fabrizi, *Chem. Rev.*, 2005, **105**, 2873–2920.

4 B. Zhou, J. Du, Y. Yang and Y. Li, *Chem.–Eur. J.*, 2014, **20**, 12768–12772.

5 Y. Kim, D. Kim and S. Chang, *Chem. Commun.*, 2021, **57**, 12309–12312.

6 (*a*) L. Zheng, K. Tao and W. Guo, *Adv. Synth. Catal.*, 2021, **363**, 62–119; (*b*) A. A. Festa, L. G. Voskressensky and E. V. V. Eycken, *Chem. Soc. Rev.*, 2019, **48**, 4401–4423; (*c*) S. Jana, A. Verma, R. Kadu and S. Kumar, *Chem. Sci.*, 2017, **8**, 6633–6644; (*d*) Y.-Y. Liu, X.-Y. Yu, J.-R. Chen, M.-M. Qiao, X. Qi, D.-Q. Shi and W. Xiao, *Angew. Chem., Int. Ed.*, 2017, **56**, 9527–9531; (*e*) M. Teders, L. Pitzer, S. Buss and F. Glorius, *ACS Catal.*, 2017, **7**, 4053–4056; (*f*) A. Sagadevan, A. Ragupathi and K. C. Hwang, *Angew. Chem., Int. Ed.*, 2015, **54**, 13896–13901; (*g*) J. Zoller, D. C. Fabry, M. A. Ronge and M. Rueping, *Angew. Chem., Int. Ed.*, 2014, **53**, 13264–13268.

7 S. Maity and N. Zheng, *Angew. Chem., Int. Ed.*, 2012, **51**, 9562–9566.

8 C.-J. Wu, Q.-Y. Meng, T. Lei, J.-J. Zhong, W.-Q. Liu, L.-M. Zhao, Z.-J. Li, B. Chen, C.-H. Tung and L.-Z. Wu, *ACS Catal.*, 2016, **6**, 4635–4639.

9 (*a*) X.-Q. Hu, X. Qi, J.-R. Chen, Q.-Q. Zhao, Q. Wei, Y. Lan and W.-J. Xiao, *Nat. Commun.*, 2016, **7**, 11188; (*b*) P. J. Kocienski, *Protecting Groups*, Georg Thieme, NewYork, 3rd edn, 2005.

10 (*a*) X.-Q. Chu, D. Ge, Y.-Y. Cui, Z.-L. Shen and C.-J. Li, *Chem. Rev.*, 2021, **121**, 12548–12680; (*b*) I. A. MacKenzie, L. Wang, N. P. R. Onuska1, O. F. Williams, K. Begam, A. M. Moran, B. D. Dunietz and D. A. Nicewicz, *Nature*, 2020, **580**, 76–80; (*c*) E. Hasegawa, N. Izumiya, T. Miura, T. Ikoma, H. Iwamoto, S. Takizawa and S. Murata, *J. Org. Chem.*, 2018, **83**, 3921–3927; (*d*) J. Xuan, B.-J. Li, J.-Z. Feng, G.-D. Sun, H.-H. Ma, Z.-W. Yuan, J.-R. Chen, L.-Q. Lu and W.-J. Xiao, *Chem.–Asian J.*, 2013, **8**, 1090–1094.

11 Z.-S. Wang, Y.-B. Chen, H.-W. Zhang, Z. Sun, C. Zhu and L.-W. Ye, *J. Am. Chem. Soc.*, 2020, **142**, 3636–3644.

12 A. Joshi-Pangu, F. Lévesque, H. G. Roth, S. F. Oliver, L.-C. Campeau, D. Nicewicz and D. DiRocco, *J. Org. Chem.*, 2016, **81**, 7244–7249.

13 (*a*) N. Holmberg-Douglas and D. A. Nicewicz, *Chem. Rev.*, 2022, **122**, 1925–2016; (*b*) F. Wu, L. Wang, J. Chen, D. A. Nicewicz and Y. Huang, *Angew. Chem., Int. Ed.*, 2018, **57**, 2174–2178; (*c*) T. M. Nguyen, N. Manohar and D. A. Nicewicz, *Angew. Chem., Int. Ed.*, 2014, **53**, 6198–6201; (*d*) T. M. Nguyen and D. A. Nicewicz, *J. Am. Chem. Soc.*, 2013, **135**, 9588–9591; (*e*) A. J. Perkowski and D. A. Nicewicz, *J. Am. Chem. Soc.*, 2013, **135**, 10334–10337; (*f*) D. S. Hamilton and D. A. Nicewicz, *J. Am. Chem. Soc.*, 2012, **134**, 18577–18580.

14 L. Pitzer, F. Sandfort, F. Strieth-Kalthoff and F. Glorius, *Angew. Chem., Int. Ed.*, 2018, **57**, 16219–16223.
15 (*a*) N. L. Reed, G. A. Lutovsky and T. P. Yoon, *J. Am. Chem. Soc.*, 2021, **143**, 6065–6070; (*b*) J.-C. Xiang, Q. Wang and J. Zhu, *Angew. Chem., Int. Ed.*, 2020, **59**, 21195–21202; (*c*) H. Wang, Y. Man, Y. Xiang, K. Wang, N. Li and B. Tang, *Chem. Commun.*, 2019, **55**, 11426–11429.
16 T. M. Monos, R. C. McAtee and C. R. J. Stephenson, *Science*, 2018, **361**, 1369–1373.
17 C. Zou, J. B. Miers, R. M. Ballew, D. D. Dlott and G. B. Schuster, *J. Am. Chem. Soc.*, 1991, **11**, 7823–7825.
18 (*a*) L. Buzzetti, G. E. M. Crisenza and P. Melchiorre, *Angew. Chem., Int. Ed.*, 2019, **58**, 3730–3747; (*b*) M. A. Cismesia and T. P. Yoon, *Chem. Sci.*, 2015, **6**, 5426–5434.
19 X.-K. Jiang, *Acc. Chem. Res.*, 1997, **30**, 283–289.
20 X. Creary, M. E. Mehrsheikh-Mohammadi and S. J. McDonald, *J. Org. Chem.*, 1987, **52**, 3254–3263.
21 M. J. Frisch, G. W. Trucks, H. B. Schlegel, G. E. Scuseria, M. A. Robb, J. R. Cheeseman, G. Scalmani, V. Barone, G. A. Petersson, H. Nakatsuji, X. Li, M. Caricato, A. V. Marenich, J. Bloino, B. G. Janesko, R. Gomperts, B. Mennucci, H. P. Hratchian, J. V. Ortiz, A. F. Izmaylov, J. L. Sonnenberg, D. Williams-Young, F. Ding, F. Lipparini, F. Egidi, J. Goings, B. Peng, A. Petrone, T. Henderson, D. Ranasinghe, V. G. Zakrzewski, J. Gao, N. Rega, G. Zheng, W. Liang, M. Hada, M. Ehara, K. Toyota, R. Fukuda, J. Hasegawa, M. Ishida, T. Nakajima, Y. Honda, O. Kitao, H. Nakai, T. Vreven, K. Throssell, J. A. Montgomery Jr., J. E. Peralta, F. Ogliaro, M. J. Bearpark, J. J. Heyd, E. N. Brothers, K. N. Kudin, V. N. Staroverov, T. A. Keith, R. Kobayashi, J. Normand, K. Raghavachari, A. P. Rendell, J. C. Burant, S. S. Iyengar, J. Tomasi, M. Cossi, J. M. Millam, M. Klene, C. Adamo, R. Cammi, J. W. Ochterski, R. L. Martin, K. Morokuma, O. Farkas, J. B. Foresman, and D. J. Fox, *Gaussian 16*, Revision A.03, Gaussian, Inc., Wallingford CT, 2016.
22 C. Y. Legault, *CYLview*, 1.0b**https://www.cylview.org**, Université de Sherbrooke, 2009.
23 S. Kozuch and S. Shaik, *Acc. Chem. Res.*, 2011, **44**, 101–110.
24 (*a*) R. Sanz, M. P. Castroviejo, V. Guilarte, A. Pérez and F. J. Fañanás, *J. Org. Chem.*, 2007, **72**, 5113–5118; (*b*) J. R. Donald and R. J. K. Taylor, *Synlett*, 2009, **1**, 59–62.
25 H. H. Hoppe, A. Kerkenaar and A. K. Sijpesteijn, *Pestic. Biochem. Physiol.*, 1976, **6**, 413–421.
26 (*a*) R. K. Tiwari, A. K. Verma, A. K. Chhillar, D. Singh, J. Singh, V. K. Sankar, V. Yadav, G. L. Sharma and R. Chandra, *Bioorg. Med. Chem.*, 2006, **14**, 2747–2752; (*b*) R. K. Tiwari, J. Singh, A. K. Verma, D. Singh and R. Chandra, *Tetrahedron*, 2005, **61**, 9513–9518.
27 Y.-T. Tian, Y.-W. Zong, J. Nie, F.-G. Zhang and J.-A. Ma, *J. Fluorine Chem.*, 2019, **226**, 109361–109367.
28 N. K. Kaushik, N. Kaushik, P. Attri, N. Kumar, C. H. Kim, A. K. Verma and E. H. Choi, *Molecules*, 2013, **18**, 6620–6662.